



## **Influence of Layering Sequence and Thickness Distribution on the Low-Velocity Impact Response of Glass/Carbon Hybrid Laminates**

Shilpa Ramasagara Srinivasa Rao<sup>1\*</sup>, Jyothilakshmi Ramaswamy<sup>1</sup>,  
Pranesh Kudurebyalya Gopalakrishnamurthy<sup>2</sup>

<sup>1</sup> Department of Mechanical Engineering, Ramaiah Institute of Technology, Bangalore 560054, India

<sup>2</sup> Department of Mechanical Engineering, Akash Institute of Engineering and Technology, Bengaluru 562110, India

Corresponding Author Email: [shilpars1519@gmail.com](mailto:shilpars1519@gmail.com)

Copyright: ©2026 The authors. This article is published by IIETA and is licensed under the CC BY 4.0 license (<http://creativecommons.org/licenses/by/4.0/>).

<https://doi.org/10.18280/rcma.360317>

### **ABSTRACT**

**Received:** 11 April 2026  
**Revised:** 9 June 2026  
**Accepted:** 16 June 2026  
**Available online:** 30 June 2026

#### **Keywords:**

*low-velocity impact, absorbed energy, brittle behavior, stiffness, peak force, delamination*

This study investigated the low-velocity impact (LVI) response of glass fibre and carbon fibre reinforced epoxy hybrid laminates with varying stacking sequences and thickness distributions. Bidirectional woven laminates were fabricated using vacuum bagging and subjected to instrumented drop-weight impact tests at a constant impact energy of 8 J, following ASTM D7136 standards. Four configurations were analysed: (A8-A12) outer layer constant (glass) with varying core layer; (B8-B12) outer layers constant (carbon) — varying the inner layer thickness; (C8-C12) inner layers constant (carbon) with varying outer Glass layer thickness; (D8-D12) inner layers constant (glass) — varying outer carbon layer thickness. The impact response and damage characteristics were subsequently compared to establish design-oriented guidelines for hybrid laminate development. Carbon face plies increased peak load and stiffness, whereas glass face plies promoted longer contact duration and higher energy dissipation. Damage area analysis further showed that carbon face plies effectively limited both front- and back-side cracking, while glass-dominant laminates suffered enlarged damage zones. The findings provide initial design indications for tailoring glass/carbon hybrid laminates where a balance between stiffness, energy absorption, and damage resistance is required. Overall, balanced hybrid configurations with moderate ply counts, 8–10 layers, offered the most favorable, making them promising for aerospace and automotive applications where impact resistance and structural reliability are critical.

## **1. INTRODUCTION**

Composite materials play a critical role in modern engineering applications such as aerospace, automotive, marine, and biomedical sectors due to their superior specific mechanical performance combined with low structural weight. The growing demand for high-performance and lightweight structures has led to a substantial increase in the use of advanced composite systems, particularly fibre reinforced polymers (FRPs). These materials are widely recognized for their ability to achieve higher strength levels while maintaining minimal mass, making them suitable for load-bearing applications where weight efficiency is a key design requirement.

In addition to their favorable mechanical characteristics, FRP composites offer several functional advantages, including excellent corrosion resistance, reduced maintenance requirements, ease of fabrication, and long-term durability. As a result, their application has expanded across multiple industries, ranging from transportation and marine structures to infrastructure and construction. In civil engineering, FRPs are commonly utilized in reinforcement bars, sandwich panels,

and strengthening or retrofitting of existing structures, where they contribute to enhanced service life and improved structural performance [1].

Among the different categories of fibre-reinforced composites, carbon fibre reinforced polymers (CFRPs) and glass fibre reinforced polymers (GFRPs) are increasingly adopted in aerospace, automotive, and marine applications due to high specific strength, low density, and favorable resistance to impact loading. During service conditions, composite laminates are frequently subjected to impact events spanning a wide range of velocities, from low-velocity accidental impacts to high-velocity dynamic loading, which can significantly influence their damage behavior and structural integrity [2].

CFRPs, GFRPs, and their hybrid composite variants are among the most extensively utilized advanced materials due to their higher strength-to-weight ratio, corrosion resistance, and adaptability in structural design. Thus, these attributes render them particularly attractive for aerospace and automotive applications, where the demand for lightweight yet dependable materials is paramount. Despite these advantages, composite structures are prone to impact loading during service, which

can initiate damage and progressively degrade structural integrity [3].

Although hybrid composite laminates are well established and widely valued within the aerospace and automotive sectors for their multifunctional benefits, they remain vulnerable to impact events encountered during operational conditions. Such impacts often result in reductions in laminate stiffness and residual strength. The low-velocity impact (LVI) response of composites is governed by multiple parameters, including geometry, mass, and velocity of the impactor, as well as the mechanical characteristics of the reinforcing fibres, matrix system, and the stacking architecture of the laminate.

The stacking sequence employed in fibre-reinforced hybrid laminates plays a decisive role in controlling energy absorption capability and deformation behavior under impact loading. Studies have shown that positioning glass fibre plies closer to the laminate surfaces, or modifying the relative volume fractions of glass and carbon fibres, can significantly enhance the impact energy absorption of the structure. Likewise, the tensile failure behavior of hybrid composites is strongly dependent on hybrid configuration, ply orientation, and the nature of the reinforcing fibres used [4].

Hybrid composite systems provide engineers with the flexibility to tailor material properties for specific functional requirements, offering performance combinations that are difficult to achieve using single-fibre composites. Carbon fibres contribute higher stiffness, excellent strength, and low density, while glass fibres exhibit greater strain-to-failure and improved damage tolerance [5]. When these fibres are combined using an optimized stacking sequence, effective hybridization can be achieved, resulting in balanced mechanical performance [6]. From an economic perspective, partial substitution of carbon fibres with lower-cost reinforcements such as E-glass offers notable cost advantages, particularly for civil and defence aerospace applications. Hitchen and Kemp [7] proposed a cost-effective hybrid carbon fibre composite configuration & systematically examined the influence of the ply sequencing on its mechanical response and low-energy impact resistance.

Unintended low-energy impact events—such as tool drops during maintenance, airborne debris strikes, or hailstone impacts—can cause localized damage and significantly reduce the load-bearing capacity of composite structures. Depending on impact severity, damage may range from superficial surface indentation to extensive internal damage or complete perforation. The present study focuses on evaluating the influence of stacking sequence and ply orientation relative to the principal material axis on the mechanical response of hybrid laminates subjected to impact loading. Common damage modes observed in impacted composite laminates include fibre breakage, matrix cracking, fibre–matrix debonding, and delamination, with delamination being particularly harmful due to its pronounced effect on stiffness and strength degradation [8].

Unlike conventional single-fibre composites, hybrid fibre-reinforced laminates exhibit a characteristic phenomenon referred to as the hybrid effect [9]. Early investigations by Bunsell and Harris [10] and Phillips [11] first identified this effect, demonstrating notable improvements in impact resistance for symmetrically alternating carbon/glass FRP laminates. Since then, research on hybridization strategies aimed at enhancing the impact performance of FRP structures has expanded considerably. Papa et al. [12] reported that placing glass fibre layers on the impact-facing surface of

hybrid laminates further improves impact resistance, as continuous glass plies on the impacted side increase both peak load capacity and absorbed energy, but the stacking sequence was not varied with the face plies and core compositions.

The mechanical response of GFRP laminates is predominantly influenced by fibre orientation, while their through-thickness strength and toughness remain comparatively low [13]. As a result, under transverse dynamic loading conditions, LVI emerges as a critical design consideration for aerospace composite structures [14]. Such impact events can activate damage mechanisms, including delamination, matrix cracking, and fibre fracture, all of which substantially diminish residual structural performance. Consequently, considerable research has focused on understanding and improving the low-velocity impact behavior of composite laminates. Researchers have examined the effect of stacking sequence in composite laminates and showed that laminate architecture significantly affects impact damage evolution, peak load response, and failure mechanisms [15]. Experimental investigations on cross-ply and angle-ply glass/epoxy laminates subjected to varying impact energies have shown that lower impact energies predominantly induce matrix cracking and delamination, whereas higher impact energies tend to promote fibre-dominated failure modes [16].

Researchers have employed optimization approaches to improve the impact performance of hybrid fibre laminates and highlighted the importance of balancing stiffness and damage tolerance. Although these studies established the significance of stacking sequence, most investigations focused on overall hybrid ratios, optimization strategies, or specific laminate architectures. Comparatively fewer studies have systematically separated the influence of face-sheet material from the influence of through-thickness material distribution in woven glass/carbon hybrid laminates. The present work addresses this gap through four distinct laminate configurations (A–D), enabling independent assessment of (i) the effect of carbon and glass face plies on impact response and (ii) the effect of material distribution between the laminate faces and core on damage development. This approach provides design-oriented insight into how hybrid architecture governs impact behavior [17].

## 2. EXPERIMENTAL PROCEDURE

### 2.1 Materials

In this process of study, we have chosen bidirectional woven glass and carbon hybrid composite laminates, featuring fibres oriented at  $0^\circ$  and  $90^\circ$ , which were systematically evaluated under LVI loading. This architecture enhances in-plane isotropy, where certain critical applications are subject to unpredictable impact energies.

These glass-carbon hybrid composite laminates bring a well-rounded blend of structural performance, toughness, and cost efficiency. These hybrids outperform pure carbon in impact resistance and offer tailored mechanical properties for diverse environments—making them highly suitable for both research and industrial applications.

Tailored fibre placement techniques allow carbon fibre to be placed precisely where high stiffness is required, while glass fibre fills less critical areas, optimizing material use and cost. Carbon fibre is strong but brittle, whereas glass fibre is

tougher and more ductile. Hybrid composites combine these traits to reduce the brittleness of carbon, improving impact resistance and preventing catastrophic failure. In impact tests, hybrids with optimized fibre ratios absorbed more energy and reduced damage severity compared to pure carbon composites [18]. A study on glass carbon hybrids showed an improvement in impact strength versus plain carbon composites, with significantly less brittle failure. The fibre cloth is layered sequentially, with each layer by an application of the Epoxy resin (LY556) and hardener (HY951) in a ratio of 10:1 resin to hardener procured from Herenba Instruments and Engineers, Chennai, and the glass and carbon fibres are procured from The Bhor Chemicals and Plastics Pvt. Ltd, Mumbai, India, and Marktech Composites, Bangalore. The characteristics of the glass fibres and carbon fibres are given in Table 1.

**Table 1.** Material characteristics and specifications

Characteristic	Carbon Fibre	Glass Fibres
Areal Weight (g/m <sup>2</sup> )	200	200
Standard Width (mm)	1000 ± 10 mm	1000 ± 10 mm
Dry Fabric Thickness (mm)	0.2 ± 0.05 mm	0.2 ± 0.05 mm
Density (g/cm <sup>3</sup> )	1.8 min.	2.63 min.
Filament Diameter (µm)	7 nominal	13 nominal
Tensile Strength (MPa)	4000 min.	3750 min.
Tensile Modulus (GPa)	240 min.	70 min.
Elongation (%)	1.8 max.	4.8 max.
Sizing	Epoxy Compatible	Epoxy Compatible

## 2.2 Fabrication process

Composite laminates were fabricated using the vacuum bagging technique, a widely adopted process for producing high-quality, lightweight composite structures. In this method, a vacuum pump is employed to evacuate entrapped air and consolidate the fibre-resin system, thereby enhancing fibre wet-out and ensuring uniform compaction during the curing process. The fabrication of glass fibres and carbon fibre reinforced epoxy laminates was carried out under controlled vacuum conditions to minimize void content and achieve consistent laminate quality.

The laminates were manufactured with varying ply counts in accordance with ASTM D7136 specifications for LVI testing. Accordingly, bidirectional glass and carbon fibre laminates comprising 8, 10, and 12 layers were produced. The corresponding stacking sequences of the fabricated laminates are presented in Figure 1.

During the vacuum bagging process, the fabrication surface (granite slab) was thoroughly cleaned to ensure a dust-free environment. A thin layer of release agent was applied onto the surface in order to prevent adhesion of the laminate to the mould. Epoxy resin (LY556) and hardener (HY951) were then mixed in a weight ratio of 10:1 and uniformly spread over the prepared surface. The laminate dimensions were defined based on the available mould area and fixed at 500 mm × 550 mm.

Glass and carbon fibre fabrics, pre-cut to the specified dimensions, were sequentially placed onto the resin-coated surface. Resin application and fabric placement were repeated until the desired number of layers was achieved. After the placement of each ply, a bubble-bursting roller (RL52-19150, Tools4FRP, Haryana, India) was used to eliminate entrapped air and minimize void formation during lay-up.

Upon completion of the lay-up according to the prescribed

stacking sequence, a peel ply was placed over the topmost fibre layer, followed by a release film and a vacuum bagging film. The entire assembly was sealed using vacuum sealant tape to ensure airtight conditions. A vacuum pump with a capacity of 12 cubic feet per minute (CFM) was connected to evacuate air from the system, facilitating laminate consolidation and removal of excess resin, which was absorbed by the breather fabric. Vacuum was maintained for approximately two hours, after which the laminates were allowed to post-cure under ambient conditions for 24 hours.

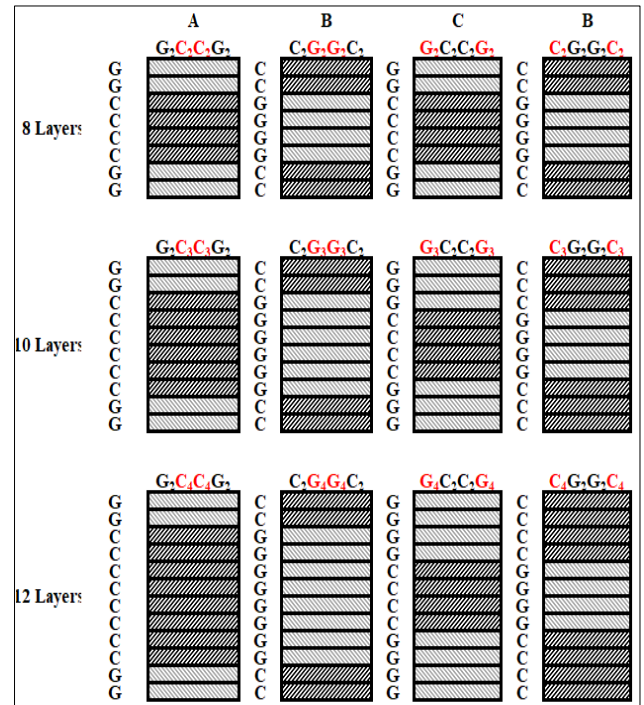


**Figure 1.** Stacking sequence with four conditions

Note: G – glass fibres and C – carbon fibres.

After curing, the fabricated laminates were cut into test specimens using a waterjet cutting machine (OM Waterjet Cutting Industry, Peenya, Bengaluru, India) in accordance with ASTM D7136 standards, with specimen dimensions of 150 mm × 100 mm. Specimen nesting was performed using Deepnest.io software to optimize material utilization. Fabrication consistency was ensured by strictly adhering to the above-described procedure. The measured laminate thickness corresponding to different ply counts is summarized in Table 2.

In this study, hybrid composites are fabricated with the above-mentioned number of layers with different combinations of glass and carbon fibres. The layering configurations are shown in Table 2. In the layering configurations, it is observed that there is an increase in the thickness of the composite laminates. In this regard, we can observe that there are four configurations. In configurations A and B, the outer layers are kept constant, and the inner layers are increased. In configurations C and D, inner layers are kept constant, and outer layers are increased to 8 layers, 10 layers, and 12 layers, respectively. The sequences G<sub>2</sub>C<sub>2</sub>G<sub>2</sub> and C<sub>2</sub>G<sub>2</sub>G<sub>2</sub>C<sub>2</sub> represent the 8-layer configurations for both the constant-face and constant-core conditions, as shown in the four stacking configurations.

Based on the laminate dimensions, fabric areal density, and measured specimen mass, the fibre volume fraction of the

fabricated hybrid laminates was estimated to lie between 42% and 46%. The slight increase with ply count is attributed to improved fibre packing within the laminate structure. However, void content was not experimentally quantified through density measurements or resin burn-off techniques

and is therefore not reported. Future work will focus on determining fibre volume fraction and void content using standardized characterization procedures to establish a more comprehensive correlation between laminate quality and impact performance.

**Table 2.** Layering configurations of hybrid glass and carbon composite laminates

Configuration	Ply Count	Sequence	Thickness (mm)	Mass (g)	Carbon (%)	Glass (%)
A8	8	G <sub>2</sub> C <sub>2</sub> C <sub>2</sub> G <sub>2</sub>	2.1	42	50	50
A10	10	G <sub>2</sub> C <sub>3</sub> C <sub>3</sub> G <sub>2</sub>	2.3	51	60	40
A12	12	G <sub>2</sub> C <sub>4</sub> C <sub>4</sub> G <sub>2</sub>	2.42	59	67	33
B8	8	C <sub>2</sub> G <sub>2</sub> G <sub>2</sub> C <sub>2</sub>	2.1	42	50	50
B10	10	C <sub>2</sub> G <sub>3</sub> G <sub>3</sub> C <sub>2</sub>	2.3	51	40	60
B12	12	C <sub>2</sub> G <sub>4</sub> G <sub>4</sub> C <sub>2</sub>	2.42	59	33	67
C8	8	G <sub>2</sub> C <sub>2</sub> C <sub>2</sub> G <sub>2</sub>	2.1	42	50	50
C10	10	G <sub>3</sub> C <sub>2</sub> C <sub>2</sub> G <sub>3</sub>	2.3	50.8	40	60
C12	12	G <sub>4</sub> C <sub>2</sub> C <sub>2</sub> G <sub>4</sub>	2.42	60.8	33	67
D8	8	C <sub>2</sub> G <sub>2</sub> G <sub>2</sub> C <sub>2</sub>	2.1	42	50	50
D10	10	C <sub>3</sub> G <sub>2</sub> G <sub>2</sub> C <sub>3</sub>	2.3	51	60	40
D12	12	C <sub>4</sub> G <sub>2</sub> G <sub>2</sub> C <sub>4</sub>	2.42	60.8	67	33

Note: G – glass fibres and C – carbon fibres.

### 3. DROP WEIGHT IMPACT TESTING

Figure 2 shows the instrumented drop weight testing machine, manufactured by SS Instruments, Bangalore, which was utilized for impact testing. The machine’s specifications are outlined in Table 3. To achieve consistent and secure positioning, the laminate was fastened using four toggle clamps. Additionally, an anti-rebound mechanism was integrated into the setup to prevent multiple impacts on the specimen. The testing apparatus included a 12.7 mm diameter hemispherical striker, attached to a tup weighing 4 kg, and the height of fall of the impactor was set as 198 mm as per the setting of the drop weight testing machine.

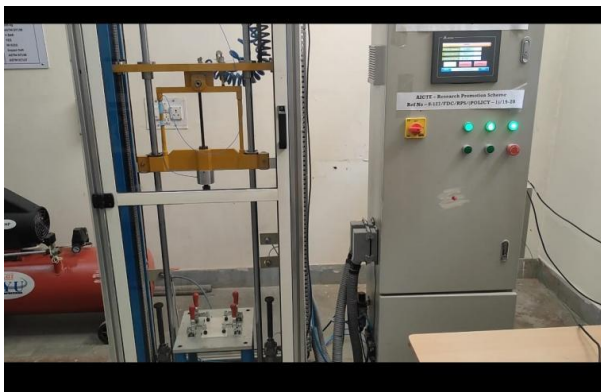


**Figure 2.** Drop weight testing machine

**Table 3.** Specifications of drop weight testing machine

Description	Parameters
Drop Height	0.2 m–1.5 m
Weight of Tup	4 kg–30 kg
Impactor Type	Hemispherical (φ12.7 mm)
Velocity	1.98–5.42 m/sec
Impact Energy	8 J–441 J
Machine Weight	650 kg
Test Area Dimension	ASTM D7136
Compressed Air Supply	4 BAR
Anti-rebound Mechanism	YES
DAC System	NI 6210
Software System	Impact Soft

### 3.1 Energy analysis

The impact energy characteristics were evaluated using data obtained from the instrumented drop-weight impact testing system. For all specimens, the initial impact energy was maintained at 8 J and calculated from the mass of the impactor and the selected drop height using the following relationship in Eq. (1):

$$E_i = mgh \quad (1)$$

where,  $m$  denotes the impactor mass,  $g$  is the acceleration due to gravity, and  $h$  represents the drop height.

The absorbed energy ( $E_a$ ) refers to the portion of the impact energy consumed by damage mechanisms within the laminate, including matrix cracking, fibre breakage, fibre–matrix interface separation, and delamination [3].

The elastic or rebound energy ( $E_r$ ) represents the amount of energy returned by the specimen during impactor rebound [19]. It was calculated as the difference between the initial impact energy and the absorbed energy, as shown in Eq. (2):

$$E_r = E_i - E_a \quad (2)$$

Based on the conservation of energy, the relationship between the impact energy components is given by Eq. (3):

$$E_i = E_a + E_r \quad (3)$$

In this study, the incident impact energy ( $E_i$ ) was kept constant at 8 J for all tested laminate configurations.

## 4. RESULTS AND DISCUSSIONS

Table 4 shows the energy absorption performance of hybrid composite laminates subjected to an 8 J LVI, evaluated under four stacking strategies or configurations,

- A. Outer layers constant (glass) with varying inner carbon layer thickness
- B. Outer layers constant (carbon) — varying the inner layer thickness
- C. Inner layers constant (carbon) with varying outer

D. Inner layers constant (glass) — varying outer carbon

**Table 4.** Consolidated results of hybrid specimens for 8 J impact energy

Stacking Condition	Configurations	Stacking Sequences	Ply Counts	Absorbed Energy (J)	Elastic Energy (J)	Peak Force (kN)	Displacement (mm)	Contact Duration (ms)
Outer layer is constant & inner layer is increasing	A8	G <sub>2</sub> C <sub>2</sub> C <sub>2</sub> G <sub>2</sub>	8	7.6	0.4	2	10.2	11.0
	A10	G <sub>2</sub> C <sub>3</sub> C <sub>3</sub> G <sub>2</sub>	10	6.8	1.2	2.115	6.8	11.3
	A12	G <sub>2</sub> C <sub>4</sub> C <sub>4</sub> G <sub>2</sub>	12	5.5	2.5	2.485	6.1	13.1
	B8	C <sub>2</sub> G <sub>2</sub> G <sub>2</sub> C <sub>2</sub>	8	7.4	0.6	1.5	10.4	10.1
	B10	C <sub>2</sub> G <sub>3</sub> G <sub>3</sub> C <sub>2</sub>	10	0.2	7.8	3.17	5.8	10.4
	B12	C <sub>2</sub> G <sub>4</sub> G <sub>4</sub> C <sub>2</sub>	12	0.1	7.9	3.285	4.9	8.9
Outer layers are increasing & inner layer is constant	C8	G <sub>2</sub> C <sub>2</sub> C <sub>2</sub> G <sub>2</sub>	8	7.6	0.4	2	10.2	11.0
	C10	G <sub>3</sub> C <sub>2</sub> C <sub>2</sub> G <sub>3</sub>	10	3.5	4.5	2.465	5.8	11.1
	C12	G <sub>4</sub> C <sub>2</sub> C <sub>2</sub> G <sub>4</sub>	12	1.3	6.7	2.905	4.8	10.0
	D8	C <sub>2</sub> G <sub>2</sub> G <sub>2</sub> C <sub>2</sub>	8	7.4	0.6	1.5	10.4	10.1
	D10	C <sub>3</sub> G <sub>2</sub> G <sub>2</sub> C <sub>3</sub>	10	6.8	1.2	2.44	7.0	11.3
	D12	C <sub>4</sub> G <sub>2</sub> G <sub>2</sub> C <sub>4</sub>	12	5	3	2.745	6.0	11.4

Note: G – glass fibres and C – carbon fibres.

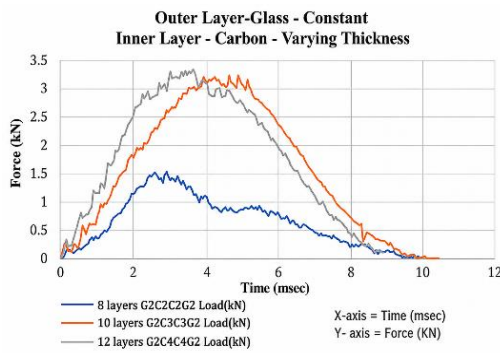
**4.1 Outer layers constant (glass) with varying inner carbon layer thickness**

When the outer layers were kept constant as glass with varying inner carbon layers, i.e., G<sub>2</sub>C<sub>2</sub>C<sub>2</sub>G<sub>2</sub> (8), G<sub>2</sub>C<sub>3</sub>C<sub>3</sub>G<sub>2</sub> (10), G<sub>2</sub>C<sub>4</sub>C<sub>4</sub>G<sub>2</sub> (12), a progressive reduction in absorbed energy was observed as the carbon content increased, decreasing sharply from 7.4 J at 8 layers to only 0.1 J at 12 layers, as in Figure 3(a). Concurrently, elastic energy increased, indicating that most of the impact energy is stored elastically instead of being dissipated, and peak force increased from 1.5 kN, i.e., 8 layers, to 3.285 kN at 12 layers, along with a reduction in displacement and contact duration, as shown in Figures 3(b) and (c). This indicates that greater carbon thickness imparts high stiffness, promoting elastic storage of impact energy rather than dissipation, which compromises impact tolerance [20].

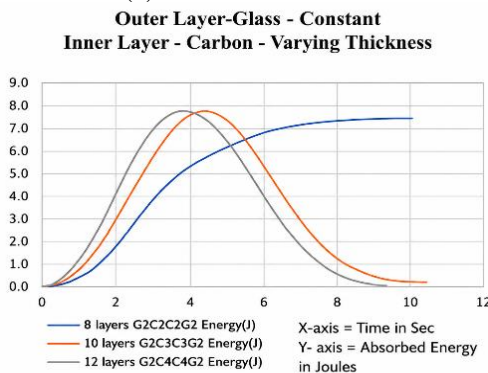


(c) Displacement vs. time

**Figure 3.** Impact response of hybrid laminates with constant glass outer layers and varying carbon inner layers



(a) Peak force vs. time



(b) Absorbed energy vs. time

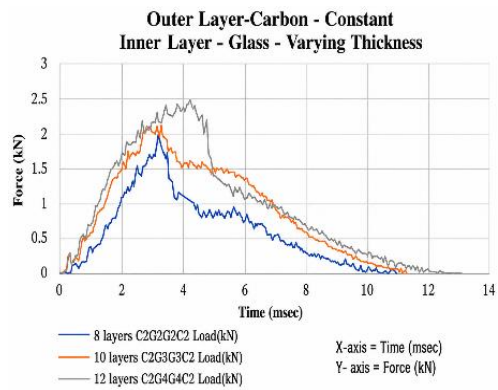
With glass on the outside and increasing carbon thickness inside, laminates become stiffer and more elastic, but their ability to absorb impact energy reduces. The system favors energy storage rather than dissipation, which may be detrimental to impact tolerance.

Keeping glass faces constant while increasing carbon in the mid-plane enhances flexural stiffness. Carbon’s high modulus allows it to carry more load, but it limits progressive damage, leading to higher peak forces but lower absorbed energy. The reduced curve width (shorter duration) in 12-ply laminates reflects lower deformation tolerance and a brittle failure mode [21].

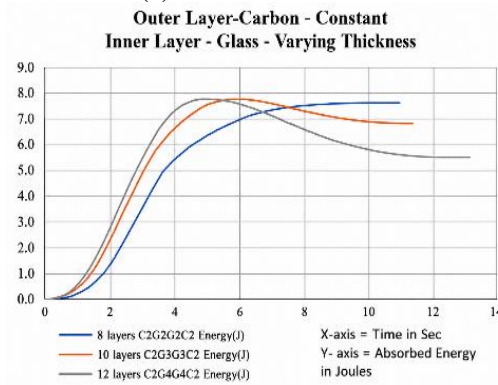
**4.2 Outer layers constant (carbon) — Varying inner layer thickness**

In the second configuration (B), the outer layers were carbon, while the inner layer thickness varied. The corresponding stacking sequences were C<sub>2</sub>G<sub>2</sub>G<sub>2</sub>C<sub>2</sub> (8 plies), C<sub>2</sub>G<sub>3</sub>G<sub>3</sub>C<sub>2</sub> (10 plies), and C<sub>2</sub>G<sub>4</sub>G<sub>4</sub>C<sub>2</sub> (12 plies). When carbon is outside and glass increases inside, the absorbed energy gradually decreases from 7.6 J at 8 layers to 5.5 J at 12 layers, and elastic energy increases progressively but not as drastically as in configuration A. There is a longer contact duration, which indicates that there is a more progressive impact response, as shown in Figures 4(a)-(c). This

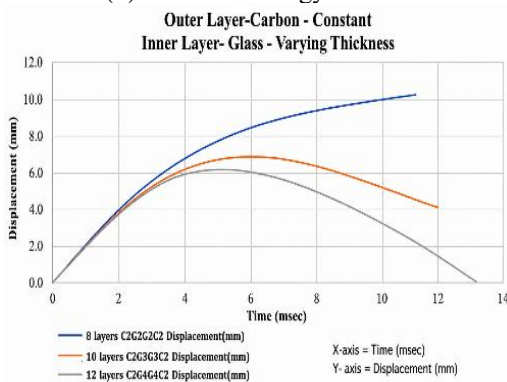
configuration provides a balance between stiffness and energy dissipation, as the outer carbon plies contribute to load resistance while the inner glass facilitates partial absorption [22].



(a) Peak force vs. time



(b) Absorbed energy vs. time



(c) Displacement vs. time

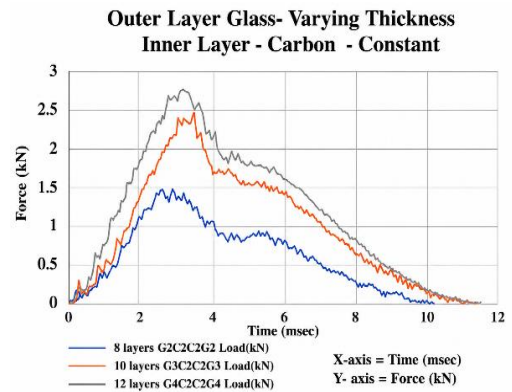
**Figure 4.** Impact response of hybrid laminates with constant carbon outer layers and varying inner glass layer thickness

Glass inner layers are more compliant and promote progressive damage modes (matrix cracking, delamination growth, fibre–matrix friction). With carbon faces providing initial stiffness, the glass core allows through-thickness deformation and distributed damage that converts impact kinetic energy into dissipative work. This gives broader, smoother load–time curves and longer contact durations. The result is improved energy absorption at the expense of peak-load carrying capacity.

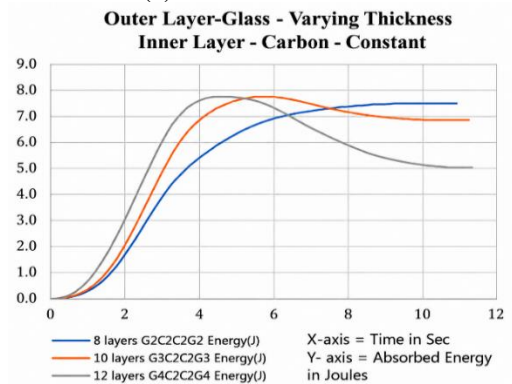
### 4.3 Inner layers constant (carbon) with varying outer glass layer thickness

The third configuration is C, where the stacking sequence is

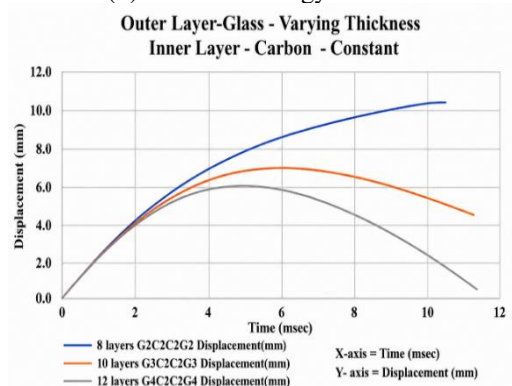
$G_2C_2C_2G_2$  (8),  $G_3C_2C_2G_3$  (10),  $G_4C_2C_2G_4$  (12). For laminates with carbon as the constant inner layer and varying glass at the outer surfaces, a similar trend of decreasing absorbed energy was recorded, reducing from 7.4 J to 5 J with increasing glass thickness. When carbon remains central, and glass is varied on the outer surfaces, the system becomes progressively stiffer, showing moderate elastic storage. However, the decline was moderate compared to carbon-dominated sequences, and contact duration remained relatively stable. Peak force increased from 1.5 kN to 2.745 kN, showing higher resistance to penetration. These results highlight that the glass outer layers contribute to delaying failure and enhancing damage tolerance, although stiffness and peak force rise with thickness (see Figures 5(a)–(c)).



(a) Peak force vs. time



(b) Absorbed energy vs. time



(c) Displacement vs. time

**Figure 5.** Impact response of hybrid laminates with varying glass outer layers and constant carbon inner layer

Glass on the surfaces promotes progressive failure mechanisms (matrix cracking, delamination), allowing higher energy absorption. Carbon mid-planes maintain the baseline stiffness, but glass outer plies dominate the impact response

by spreading damage and delaying sudden catastrophic failure. As a result, laminates with more glass face plies deform more and dissipate more energy.

#### 4.4 Inner layers constant (glass) — varying outer carbon layer thickness

Finally, the fourth configuration D, where the stacking sequences are  $C_2G_2G_2C_2$  (8),  $C_3G_2G_2C_3$  (10),  $C_4G_2G_2C_4$  (12), where the inner layers were fixed as glass with increasing outer carbon thickness. Here, absorbed energy declined steeply from 7.6 J at 8 layers to 1.3 J at 12 layers, and Elastic energy and peak force rose sharply. At the same time, displacement decreased significantly, confirming that carbon-dominant outer layers yield a stiff but brittle response with limited capacity for impact energy dissipation, as shown in Figures 6(a)-(c).

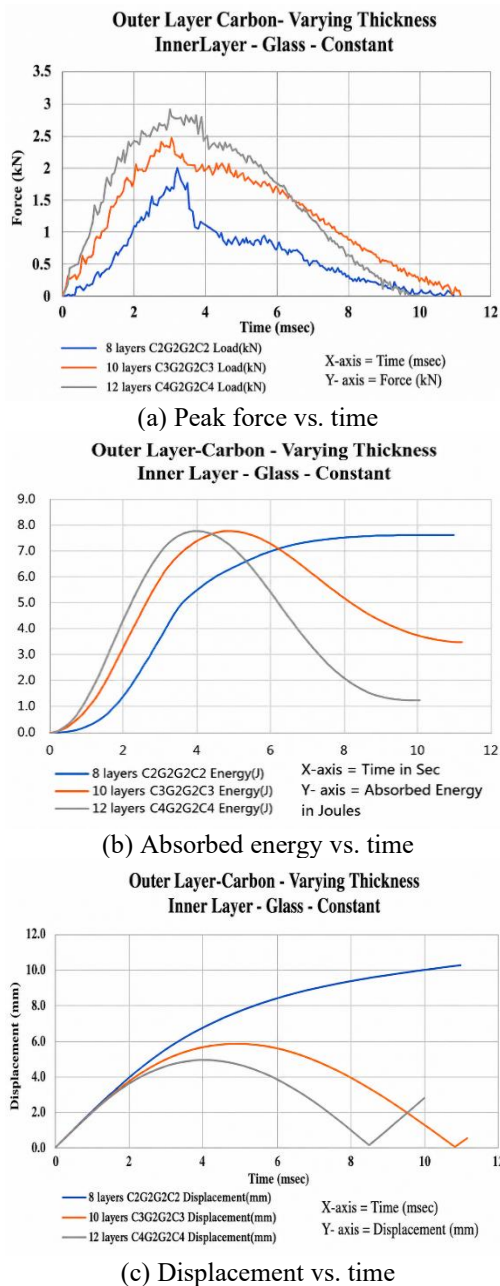


**Figure 6.** Impact response of hybrid laminates with varying carbon outer layers and constant inner layer thickness

Thick carbon face plies raise bending and surface stiffness, concentrating loads near the impact region and limiting through-thickness deformation. Carbon’s high modulus favors elastic response and localized damage (fiber fracture or sudden delamination) rather than progressive dissipative mechanisms. The result is higher peak loads and a more brittle-type load response.

#### 4.5 Similarity interpretation

(1) 8-layer laminates ( $C_2G_2G_2C_2$  and  $G_2C_2C_2G_2$ ): These specimens demonstrate almost identical responses, characterized by high energy absorption and greater flexibility, making them the most effective in terms of impact tolerance.

(2) 10-layer laminates ( $C_2G_3G_3C_2$  and  $G_3C_2C_2G_3$ ): Both configurations show a moderate performance, providing a compromise between stiffness and energy dissipation, thereby offering a balanced mechanical response under impact.

(3) 12-layer laminates ( $C_4G_2G_2C_4$  and  $G_4C_2C_2G_4$ ): These exhibit comparable trends, marked by high stiffness but brittle behavior, with minimal energy absorption. Such designs are favorable where rigidity is prioritized, but are least effective for impact energy dissipation.

#### 4.6 Cross-configuration comparison

Across all configurations in Table 5, the highest absorbed energy was observed in the 8-ply laminates, particularly  $C_2G_2G_2C_2$  and  $G_2C_2C_2G_2$ , indicating superior impact tolerance. In contrast, the smallest damage area was obtained in the carbon-face-sheet configuration  $C_4G_2G_2C_4$ , demonstrating the effectiveness of carbon outer plies in restricting surface damage propagation. These observations reveal a clear trade-off: configurations optimized for energy absorption generally exhibit larger damage zones, whereas configurations optimized for damage suppression tend to dissipate less impact energy and behave more elastically. Therefore, balanced 8–10 ply hybrid architectures provide the most favorable compromise between impact tolerance and structural stiffness.

**Table 5.** Cross-comparison of impact response and damage characteristics for hybrid laminate configurations at equal ply counts

Ply Count	Highest Absorbed Energy	Smallest Damage Area	Design Interpretation
8 Ply	$C_2G_2G_2C_2$ (7.6 J)	$G_2C_2C_2G_2$ (28.68 mm <sup>2</sup> backside)	Excellent impact tolerance Balanced
10 Ply	$C_2G_3G_3C_2$	$G_2C_3C_3G_2$	stiffness-energy response
12 Ply	$C_2G_4G_4C_2$ (energy)	$C_4G_2G_2C_4$ (23.62 mm <sup>2</sup> backside)	Stiff but brittle

Note: G – glass fibres and C – carbon fibres.

#### 4.7 Final interpretations

The results show that laminate stacking sequence and thickness distribution between glass and carbon layers strongly influence impact energy absorption and damage tolerance. When top and bottom carbon face plies are constant, increasing the inner glass thickness improves absorbed energy

and displacement but reduces peak force and elastic energy. Conversely, when top and bottom glass faces are constant, increasing the inner carbon thickness raises peak load and elastic energy but drastically reduces absorbed energy, indicating brittle failure. In laminates where the inner carbon is constant, increasing glass at the outer faces enhances absorbed energy and contact duration, leading to more progressive failure modes. On the other hand, with an inner glass constant, increasing carbon face plies significantly increases stiffness and peak force but lowers displacement and energy absorption. Eight-layer configurations  $C_2G_2G_2C_2$  and  $G_2C_2C_2G_2$  generally show the highest absorbed energy, confirming their superior damage tolerance. Twelve-layer laminates with thicker carbon or glass domination exhibit minimal absorbed energy despite higher peak loads, highlighting their brittle nature. A clear trade-off is observed:

higher carbon content provides stiffness and peak load resistance, while higher glass content promotes energy dissipation and longer contact durations. The load–time graphs support this trend, with glass-rich configurations showing broader, smoother curves, while carbon-rich laminates exhibit steep peaks and abrupt failure. Overall, balanced hybrids with moderate thickness (8–10 layers) provide the best compromise between stiffness and energy absorption, making them ideal for impact-resistant applications.

#### 4.8 Damage area

From Table 6, experimental findings clearly demonstrate that stacking sequence and ply distribution strongly influence both energy absorption and damage characteristics under LVI.

**Table 6.** Damage area of hybrid specimens

Stacking Condition	Stacking Sequences	No. of Layers	Damage Area	
			Front Side	Back Side
Outer layer constant & increasing inner layer	$C_2G_2G_2C_2$	8	88.16	73.66
	$C_2G_3G_3C_2$	10	106.78	91.05
	$C_2G_4G_4C_2$	12	131.17	78.38
	$G_2C_2C_2G_2$	8	90.9	28.68
	$G_2C_3C_3G_2$	10	44.28	40.88
	$G_2C_4C_4G_2$	12	79.64	74.57
	$C_2G_2G_2C_2$	8	88.16	73.66
Increasing outer layers & keeping inner layer constant	$C_3G_2G_2C_3$	10	81.34	97.86
	$C_4G_2G_2C_4$	12	48.64	23.62
	$G_2C_2C_2G_2$	8	90.9	28.68
	$G_3C_2C_2G_3$	10	56.74	34.87
	$G_4C_2C_2G_4$	12	34.28	33.15

When the top and bottom carbon layers were kept constant with increasing inner glass plies  $C_2G_2G_2C_2 \rightarrow C_2G_3G_3C_2 \rightarrow C_2G_4G_4C_2$ , the laminates exhibited a progressive reduction in absorbed energy, shifting from 7.4 J for 8-layer to almost negligible levels for 12-layer configurations. The corresponding load-displacement curves showed a stiffer but more brittle response, dominated by elastic energy storage. This brittle behavior was further reflected in the damage area, where the front-face cracks increased substantially from 88.16 to 131.17 mm<sup>2</sup>. Hence, glass-dominant cores contributed to poor energy dissipation and enlarged surface cracking, see Table 6.

In contrast, when the inner glass plies were held constant, and carbon plies increased at the outer surfaces  $C_2G_2G_2C_2 \rightarrow C_3G_2G_2C_3 \rightarrow C_4G_2G_2C_4$ , the absorbed energy remained moderate, 7.4 J to 5 J, but peak load capacity increased, indicating enhanced stiffness and crack resistance. The damage area reduced drastically on both the front from 88.34 to 48.64 mm<sup>2</sup> and back from 73.66 to 23.62 mm<sup>2</sup> surfaces, confirming that carbon face sheets act as effective barriers against impact-induced damage. This configuration proved most effective in suppressing delamination growth while maintaining structural rigidity.

When the top and bottom glass layers were kept constant with increasing inner carbon plies,  $G_2C_2C_2G_2 \rightarrow G_2C_3C_3G_2 \rightarrow G_2C_4C_4G_2$ , the absorbed energy decreased with additional plies, while peak load increased, signifying improved stiffness. However, due to brittle glass skins, the damage response was inconsistent: the front-face area initially decreased to 90.9 and 44 mm<sup>2</sup> but increased again at higher ply counts to 79 mm<sup>2</sup>. This suggests that inner carbon layers

improved stiffness, but the presence of glass at the outer surfaces still governed crack initiation and visible surface damage (see Table 7).

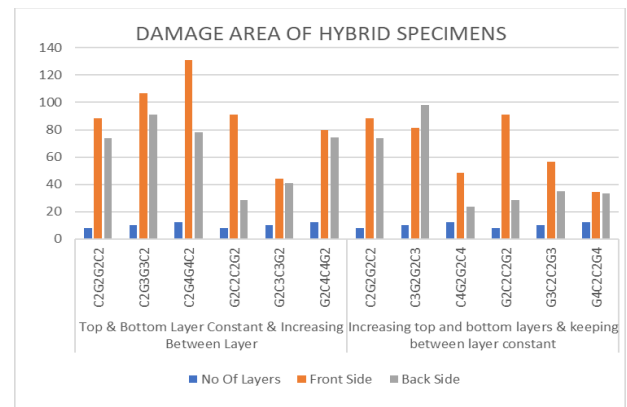


**Figure 7.** Graph of the damage area of hybrid specimens

Finally, when the inner carbon layers were kept constant with increasing glass plies on the outer surfaces  $G_2C_2C_2G_2 \rightarrow G_3C_2C_2G_3 \rightarrow G_4C_2C_2G_4$ , a gradual decrease in absorbed energy from 7.4 to 5 J was observed alongside increased stiffness. The damage analysis revealed reduced front damage from 90.9 to 34.28 mm<sup>2</sup> and a substantial increase in the back-face cracking from 28.68 to 33.15 mm<sup>2</sup>. This indicates that while glass at the outer layers is prone to visible surface cracking, the carbon core effectively restricted damage propagation through the laminate thickness, improving backside protection, as shown in Figure 7.

**Table 7.** Front and back side damage of hybrid specimens

Sl No.	Stacking Sequence	No. of Layers	Front Side Damage Image	Back Side Damage Image
1	C <sub>2</sub> G <sub>2</sub> G <sub>2</sub> C <sub>2</sub>	8		
2	C <sub>2</sub> G <sub>3</sub> G <sub>3</sub> C <sub>2</sub>	10		
3	C <sub>2</sub> G <sub>4</sub> G <sub>4</sub> C <sub>2</sub>	12		
4	G <sub>2</sub> C <sub>2</sub> C <sub>2</sub> G <sub>2</sub>	8		
5	G <sub>2</sub> C <sub>3</sub> C <sub>3</sub> G <sub>2</sub>	10		
6	G <sub>2</sub> C <sub>4</sub> C <sub>4</sub> G <sub>2</sub>	12		
7	C <sub>2</sub> G <sub>2</sub> G <sub>2</sub> C <sub>2</sub>	8		
8	C <sub>3</sub> G <sub>2</sub> G <sub>2</sub> C <sub>3</sub>	10		
9	C <sub>4</sub> G <sub>2</sub> G <sub>2</sub> C <sub>4</sub>	12		
10	G <sub>2</sub> C <sub>2</sub> C <sub>2</sub> G <sub>2</sub>	8		
11	G <sub>3</sub> C <sub>2</sub> C <sub>2</sub> G <sub>3</sub>	10		
12	G <sub>4</sub> C <sub>2</sub> C <sub>2</sub> G <sub>4</sub>	12		

Overall, increased carbon at the outer layers was most effective in limiting both front- and back-side damage while maintaining stiffness, making them suitable for applications demanding high impact resistance. Conversely, glass-dominant cores promoted brittle behavior with larger damage areas, reducing overall impact tolerance. Configurations with outer layers of glass and carbon inner layers offered a trade-off, providing excellent backside protection at the expense of

increased front-surface cracking (see Table 7).

## 5. CONCLUSIONS

This study systematically investigated the LVI response of hybrid glass/carbon fibre reinforced epoxy laminates with varying stacking sequences and thicknesses. The results consistently demonstrated that the placement of carbon or glass layers strongly governs the balance between energy absorption, stiffness, and visible damage tolerance.

- i) Carbon-rich outer layers minimized both front- and backside damage, offering superior impact tolerance.
- ii) Glass-dominant skins exhibited brittle cracks with larger front-side damage zones despite moderate absorption.
- iii) Hybrid configurations with glass skins and carbon cores provided effective backside protection but higher surface cracking.
- iv) Increasing laminate thickness enhanced stiffness but reduced energy absorption, promoting brittle failure.
- v) The findings provide initial design indications for selecting glass/carbon hybrid stacking sequences where a balance between impact energy absorption and damage suppression is required. Further validation through post-impact residual strength testing is necessary before structural design recommendations can be established.

## ACKNOWLEDGEMENT

The authors are thankful to the Department of Mechanical Engineering, Ramaiah Institute of Technology, Bangalore - 560054, for their continuous academic support. Special thanks are extended to Dr. Sunith Babu for his mentorship, insightful suggestions, and encouragement throughout the research process.

## REFERENCES

- [1] Najem, Ogunleye, R.O., Rusnakova, S., Zaludek, M., Emebu, S. (2022). The influence of ply stacking sequence on mechanical properties of carbon/epoxy composite laminates. *Polymers*, 14(24): 5566. <https://doi.org/10.3390/polym14245566>
- [2] Seifoori, S., Mahdian Parrany, A., Mirzarahmani, S. (2021). Impact damage detection in CFRP and GFRP curved composite laminates subjected to low-velocity impacts. *Composite Structures*, 261: 113278. <https://doi.org/10.1016/j.compstruct.2020.113278>
- [3] Chen, D., Luo, Q., Meng, M., Sun, G. (2019). Low velocity impact behavior of interlayer hybrid composite laminates with carbon/glass/basalt fibres. *Composites Part B: Engineering*, 176: 107191. <https://doi.org/10.1016/j.compositesb.2019.107191>
- [4] Luo, Z., Wang, H., Ng, C.T., Fu, J., Zhang, Z., Wang, C. (2024). On the low-velocity impact properties of CFRP/HAFRP interlayer hybrid fibre composite laminates. *Engineering Structures*, 315: 118387. <https://doi.org/10.1016/j.engstruct.2024.118387>
- [5] Onal, L., Adanur, S. (2002). Effect of stacking sequence on the mechanical properties of glass-carbon hybrid

- composites before and after impact. *Journal of Industrial Textiles*, 31(4): 255-272. <https://doi.org/10.1106/152808302028713>
- [6] Summerscales, J., Short, D. (1978). Carbon fibre and glass fibre hybrid reinforced plastics. *Composites*, 9(3): 157-166. [https://doi.org/10.1016/0010-4361\(78\)90341-5](https://doi.org/10.1016/0010-4361(78)90341-5)
- [7] Hitchen, S.A., Kemp, R.M.J. (1996). Development of novel cost effective hybrid ply carbon-fibre composites. *Composites Science and Technology*, 56(9): 1047-1054. [https://doi.org/10.1016/0266-3538\(96\)00064-4](https://doi.org/10.1016/0266-3538(96)00064-4)
- [8] Wang, A., Liu, X., Yue, Q., Xian, G. (2023). Effect of volume ratio and hybrid mode on low-velocity impact properties of unidirectional flax/carbon fiber hybrid reinforced polymer composites. *Thin-Walled Structures*, 187: 110764. <https://doi.org/10.1016/j.tws.2023.110764>
- [9] Lyu, Q., Wang, B., Zhao, Z., Guo, Z. (2022). Damage and failure analysis of hybrid laminates with different ply-stacking sequences under low-velocity impact and post-impact compression. *Thin-Walled Structures*, 180: 109743. <https://doi.org/10.1016/j.tws.2022.109743>
- [10] Bunsell, A.R., Harris, B. (1974). Hybrid carbon and glass fibre composites. *Composites*, 5(4): 157-164. [https://doi.org/10.1016/0010-4361\(74\)90107-4](https://doi.org/10.1016/0010-4361(74)90107-4)
- [11] Phillips, L.N. (1976). The hybrid effect — Does it exist? *Composites*, 7(1): 7-8. [https://doi.org/10.1016/0010-4361\(76\)90273-1](https://doi.org/10.1016/0010-4361(76)90273-1)
- [12] Papa, I., Boccarusso, L., Langella, A., Lopresto, V. (2020). Carbon/glass hybrid composite laminates in vinylester resin: Bending and low velocity impact tests. *Composite Structures*, 232: 111571. <https://doi.org/10.1016/j.compstruct.2019.111571>
- [13] Kurşun, A., Şenel, M., Enginsoy, H.M., Bayraktar, E. (2016). Effect of impactor shapes on the low velocity impact damage of sandwich composite plate: Experimental study and modelling. *Composites Part B: Engineering*, 86: 143-151. <https://doi.org/10.1016/j.compositesb.2015.09.032>
- [14] Shetty, H., Sethuram, D., Rammohan, B., Budarapu, P.R. (2020). Low-velocity impact studies on GFRP and hybrid composite structures. *International Journal of Advanced Engineering Sciences and Applied Mathematics*, 12(3-4): 125-141. <https://doi.org/10.1007/s12572-021-00287-9>
- [15] Hongkarnjanakul, N., Bouvet, C., Rivallant, S. (2013). Validation of low velocity impact modelling on different stacking sequences of CFRP laminates and influence of fibre failure. *Composite Structures*, 106: 549-559. <https://doi.org/10.1016/j.compstruct.2013.07.008>
- [16] K.G., P., Manjunath, A., K.C., N., Bhat, R., D., P., Bhowmik, A., Prakash, C. (2024). Influence of nanosilica on mechanical performance in woven carbon/kevlar/epoxy hybrid composites. *Journal of Engineering*, 2024(1): 2646317. <https://doi.org/10.1155/je/2646317>
- [17] Bouvet, C., Castanié, B., Bizeul, M., Barrau, J.J. (2009). Low velocity impact modelling in laminate composite panels with discrete interface elements. *International Journal of Solids and Structures*, 46(14-15): 2809-2821. <https://doi.org/10.1016/j.ijsolstr.2009.03.010>
- [18] Han, Y., Qi, Y., Liu, Y. (2025). Mechanical characterization of carbon/glass fiber hybrid composites for honeycomb-structured battery enclosures. *Applied Sciences*, 15(10): 5635. <https://doi.org/10.3390/app15105635>
- [19] K.G., Pranesh, Manjunath, A., Nagaraja, K.C., Simha, A. (2024). Influence of nanofiller addition on tensile properties in fiber reinforced polymer composites. *Futuristic Trends in Mechanical Engineering*, 3(5): 55-65. <https://doi.org/10.58532/v3bdme5p1ch6>
- [20] Rout, S., Nayak, R.K., Patnaik, S.C., Yazdani Nezhad, H. (2022). Development of improved flexural and impact performance of kevlar/carbon/glass fibers reinforced polymer hybrid composites. *Journal of Composites Science*, 6(9): 245. <https://doi.org/10.3390/jcs6090245>
- [21] Zhang, J., Chaisombat, K., He, S., Wang, C.H. (2012). Hybrid composite laminates reinforced with glass/carbon woven fabrics for lightweight load bearing structures. *Materials & Design*, 36: 75-80. <https://doi.org/10.1016/j.matdes.2011.11.006>
- [22] Xu, W., Chen, J., Cui, X., Wang, D., Pu, Y. (2024). Low-velocity impact analysis and multi-objective optimization of hybrid carbon/basalt fibre reinforced composite laminate. *Composite Structures*, 343: 118305. <https://doi.org/10.1016/j.compstruct.2024.118305>